FAULT ZONE ANALYSIS

IDENTIFYING MOTOR DEFECTS USING THE ROTOR FAULT ZONE

David L. McKinnon
PdMA Corporation

Abstract: In the last decade, advancements in motor testing technology have brought forth advances in online and offline testing. Online Current Signature Analysis (CSA) is quickly becoming a standard industry practice. Offline tests include advanced inductance measurements to analyze rotor and stator health. Using a combination of online and offline tests to form a six fault zone approach offers a more complete analysis of motor health. Power Quality focuses on the quality of the voltage and current. Power Circuit focuses on the power circuit supplying power to the motor. The Stator Fault Zone focuses on the turn-to-turn insulation and internal coil connections. The Air Gap Fault Zone refers to the quality of the air gap between the rotor and the stator. The Insulation Fault Zone refers to the winding to ground insulation. The Rotor Fault Zone refers to the health of the rotor cage and laminations. All six fault zones should be analyzed to accurately assess the overall health of a motor.

I. THE SIX FAULT ZONES

A. Power Quality

The Power Quality Fault Zone focuses on the quality of the voltage and current. The power system determines the quality of the voltage, and the load determines the quality of the current waveform. Measurements to determine power quality include Fundamental and Total RMS voltage and current, Crest Factor (CF), Total Harmonic Distortion (THD), Average Voltage, Percent Imbalance, and Harmonic Voltage Factor (HVF).

B. Power Circuit

The Power Circuit Fault Zone focuses on the conductors, connections, and components that exist from the test point downstream to the motor. Power Circuit components include circuit breakers, fuses, contactors, overloads, disconnects, lug connections, and power factor correction capacitors. Measurements used to analyze power circuit health are voltage and resistive imbalances.

C. Stator

The Stator Fault Zone refers to the turn-to-turn insulation and internal coil connections. Measurements used to analyze the stator fault zone include inductive and impedance imbalances.

D. Air Gap

The Air Gap Fault Zone refers to the air gap between the rotor and stator. There are two types of air gap faults, static and dynamic eccentricity. These faults are analyzed using Current Signature Analysis (CSA) and a modified inductance measurement known as a Rotor Influence Check (RIC) test. A RIC test is described later in this paper.

E. Insulation

The Insulation Fault Zone refers to the insulation between the windings and ground. High temperatures, age, moisture, and dirt contamination are all detrimental to insulation health. Tests used to analyze the insulation system include Resistance-To-Ground (RTG), Capacitance-To-Ground (CTG), Polarization Index (PI), Dielectric Absorption (DA), and Step Voltage.

F. Rotor

The Rotor Fault Zone refers to the condition of the rotor bars, rotor laminations, and end rings. Although only a small percentage of the motor problems, rotor faults can influence other fault zones to fail. Tests used to analyze the rotor fault zone include the In-Rush Current, Current Demodulation, CSA, RIC, and Inductive Imbalance.

II. FOCUS ON THE ROTOR FAULT ZONE

A. In-Rush Current Profiles

Normal healthy motors exhibit the current profile shown by the baseline curve in Figure 1. As rotor bars become broken, the start-up current profile changes, since less voltage is induced in the rotor cage due to the change in the effective turns ratio. The effective change in turns

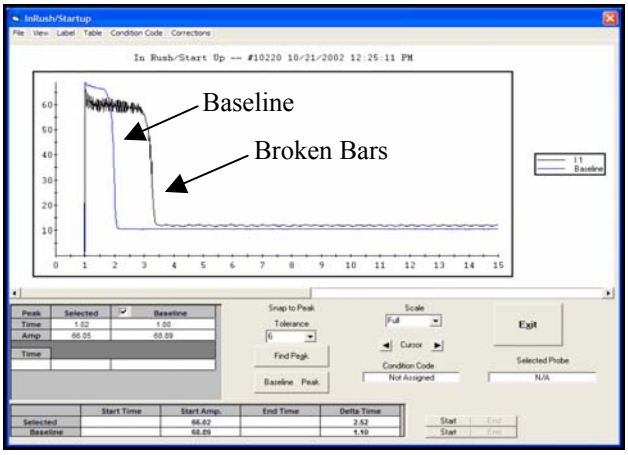

Figure 1. Varying In-Rush Profiles – Normal vs. Broken Rotor Bars

ratio results in a higher reflected impedance from the rotor to stator. Given a constant load and steady power during start-up, the higher reflected impedance lowers the amount of in-rush current as shown in the in-rush profile in Figure 1. Although the current is lower, the same total energy is required to bring the motor up to speed. With less power developed in the rotor, the time required to put the same amount of energy (Joules) into the rotor has to increase, as shown by Equation 1.

$$\text{Joule} = \text{watt} * \text{second} \qquad (1)$$

Applying Equation 2 to the rotor, it can be seen that since Torque (T) is constant, as the Power (EI) developed in the rotor decreases; the angular velocity (ω_R) must also decrease:

$$E_R I_R = \omega_R T \qquad (2)$$

Where:

E_R is the voltage developed in the rotor
I_R is the current developed in the rotor
ω_R is the angular velocity of the rotor
T is the torque developed in the rotor and is proportional to output torque

B. Steady State Current Modulation

Healthy motors with no broken rotor bars draw steady current under constant load and power system conditions. Under constant load and power system conditions, cyclical changes (sinusoidal modulations) in current may indicate a broken rotor bar using an enveloped current waveform as shown in Figure 2. Additionally, enveloped current wave-form analysis allows a technician to perform process analysis.

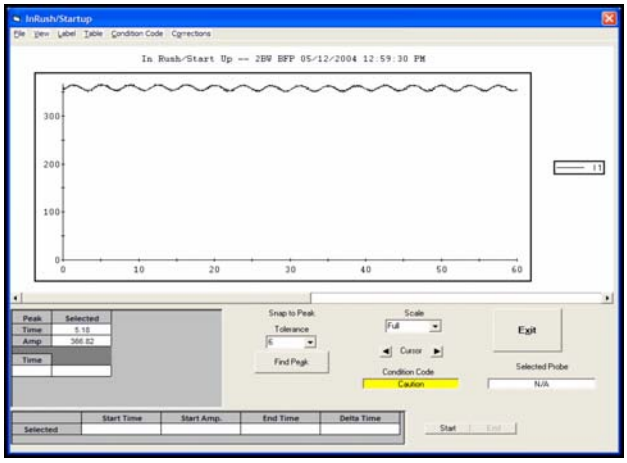
Figure 2. Current Cycling Due to Broken Rotor Bars

C. Current Demodulation

1. Mechanical Components.

Load variations are reflected into the stator currents through the motor's air gap. Current demodulation reveals repetitive load variations, thus, enhancing the ability to detect motor speed, pole-pass, mechanical pass-through, and reflected frequencies. Mechanical and reflected frequencies are related to load variances from items such as belts, gears, pumps, fans, and other mechanical components. A Fast Fourier Transform (FFT) is performed on the demodulated signal, which results in a frequency spectrum for analysis. Without demodulation, many of these load related frequencies are buried in the noise of the captured data.

2. Rotor Unbalance/Misalignment.

Utilizing current demodulation, the speed of the motor can be identified by a peak in the spectrum and monitored for changes in amplitude. A properly balanced and aligned motor has a frequency peak related to its speed that is difficult to find in the spectrum. When the motor is out of balance or misaligned, the amplitude of this peak increases. Multiples of the speed frequency develop in the demodulated current spectrum as the condition increases in severity. Figures 3 and 4 demonstrate the change in amplitude of the running speed and two times running speed during a precision alignment of a pump and motor.

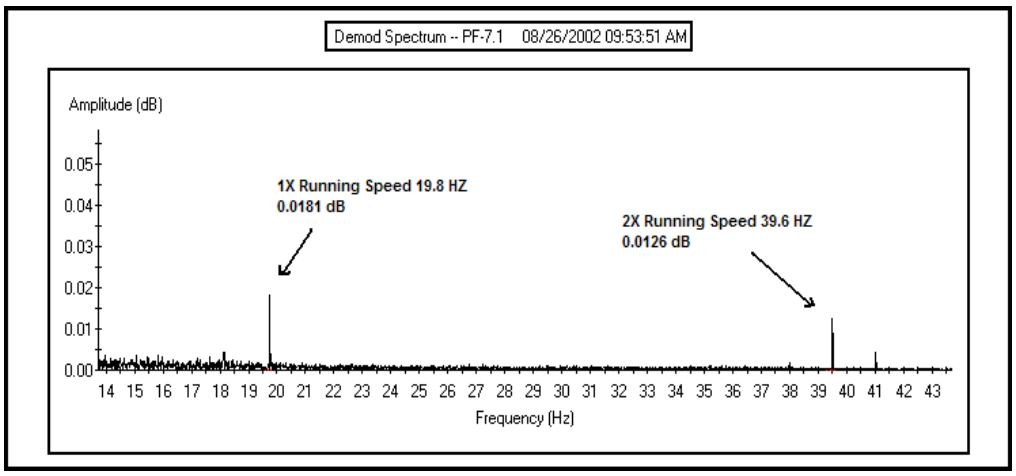

Figure 3. Demodulated Current Spectrum – Prior To Alignment

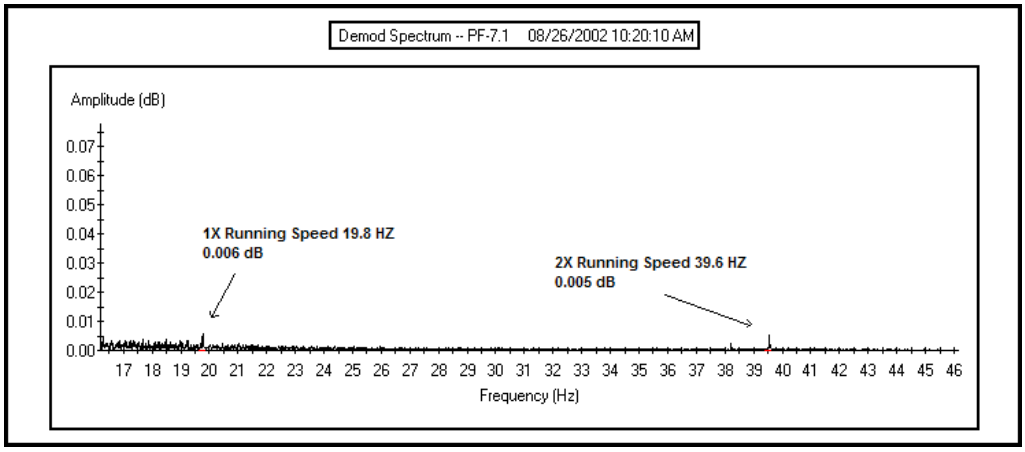

Figure 4. Current Demodulation Spectrum – After Alignment

3. Belts.

When transmitting power to the load via a belt attached to the motor, changes in belt alignment can be evaluated using the demodulated current spectrum. Increases in the amplitude of the belt frequency and the development of multiples of the belt frequency indicate a problem. The belt frequency is calculated as follows:

$$\text{Belt Frequency} = 3.142\ (D/L) \times (RPM/60) \quad (3)$$

Where:

D is diameter of the motor mounted pulley

L is the length of the belt

RPM is the motor speed

In the following example, you can see the dramatic change in the demodulated current spectrum after proper tensioning and alignment was performed on a drive belt. In Figure 5, the belt frequency is 8.188 Hz and there are elevated peaks at multiples of the belt frequency. Notice in Figure 6 the multiples of the belt frequency have disappeared and the decrease in amplitude of the belt frequency after the work was completed. These frequencies can now be easily monitored detecting possible problems developing in the belt drive of this system.

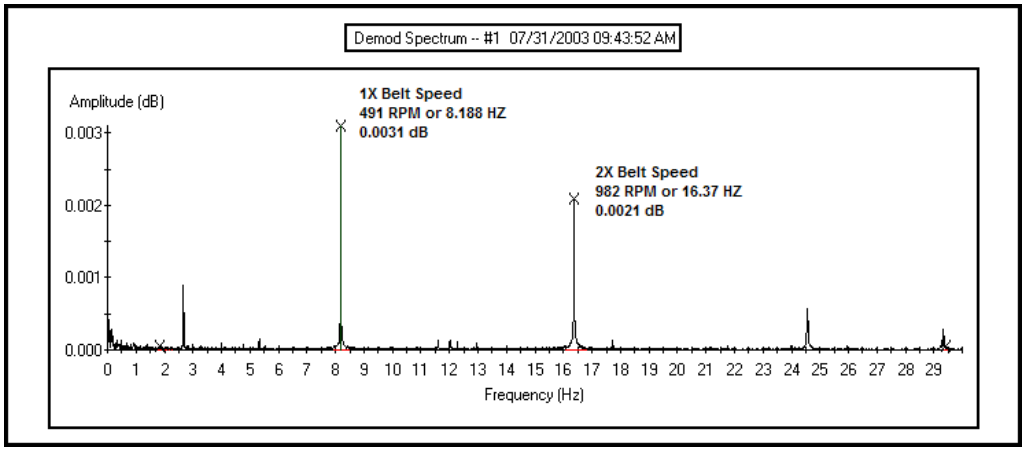

Figure 5. Demodulated Current Spectrum Prior Belt Alignment

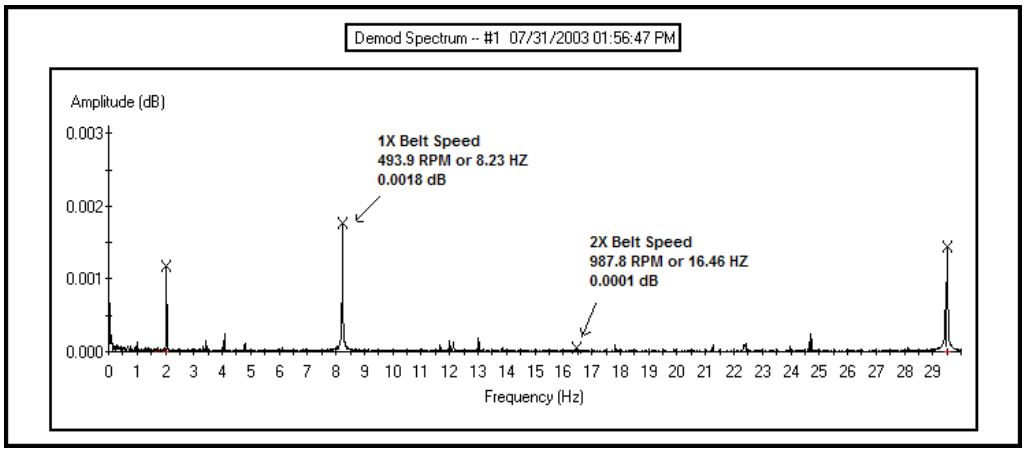

Figure 6. Current Demodulation Spectrum After Belt Alignment

4. Fans/Centrifugal Pumps.

Fan blades and centrifugal pump vane frequencies can be monitored in a demodulated current spectrum at a frequency that is equal to the number of blades (or vanes) times the pole pass frequency (F_P). Increasing amplitude at this frequency as well as a possible increase at the motor speed frequency peak is an indication of possible blade or pump vane damage. After initial installation or verification that the pump or fan is in satisfactory condition, identify the vane frequency and record the amplitude of the peak. With baseline amplitude for the equipment established, the demodulated current spectrum is used as a simple and efficient method to monitor the equipment. An example of this is seen in Figures 7 and 8, which is a comparison of two identical horizontal pumps. Figure 7 is a typical demodulated current spectrum for this application, with the pump vane frequency amplitude of 0.027 dB. In Figure 8, pump PF-8.6A pump vane frequency amplitude is 0.046 dB; nearly double that of other identical equipment platforms.

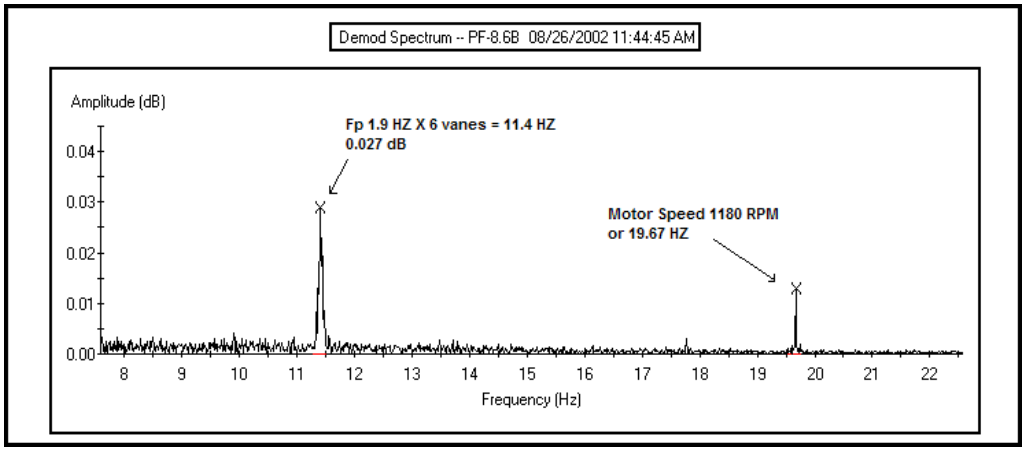

Figure 7. Typical Current Demodulation Spectrum for Several Identical Pumps

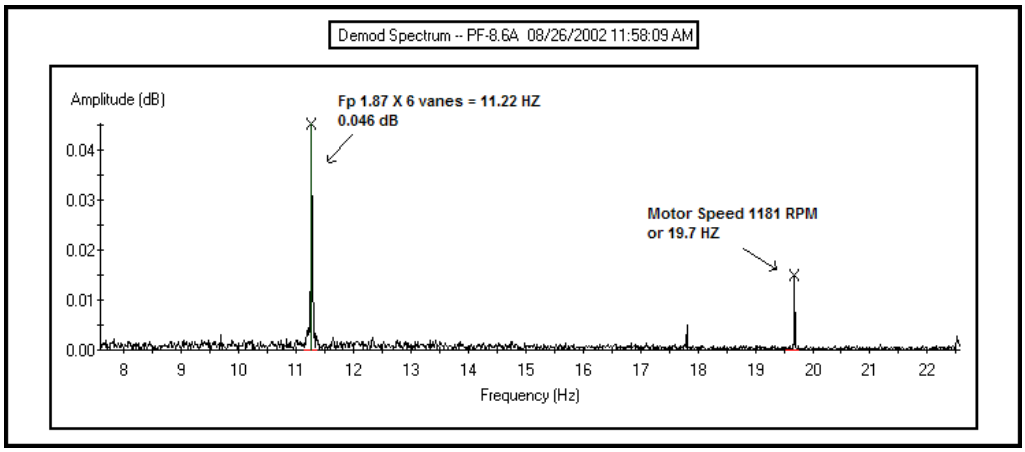

Figure 8. Current Demodulation Spectrum of Pump with Suspected Impellor Damage

D. Current Signature Analysis (CSA)

1. Pole Pass Sidebands.

A useful indicator of broken rotor bars is the pole pass sidebands around line frequency. These side bands are located in the current spectrum at (See Figure 9):

$$f_p = (1 \pm 2ks) f_{Line} \qquad (4)$$

Where:

f_p is the location of the peaks around line frequency

k is the harmonic index 1,2,3...

s is the slip

f_{Line} is the line frequency

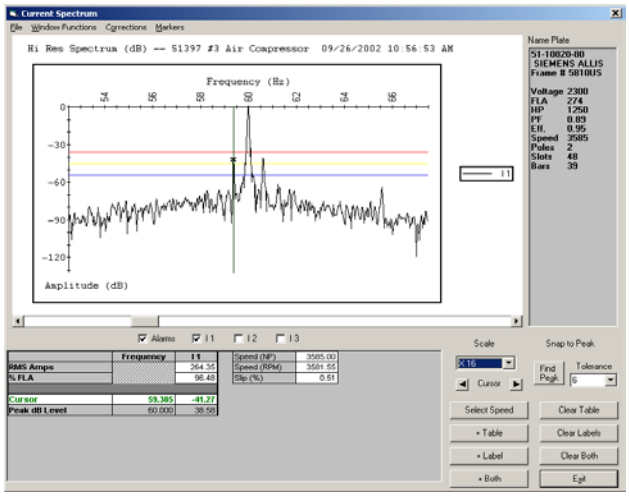

Figure 9. Pole Pass Sidebands

2. Swirl Effect.

Another useful spectral tool for detecting broken rotor bars is the swirl effect. Swirl effect occurs at the 5th harmonic of line frequency (300 Hz on a 60 Hz line frequency). See Figure 10. Swirl peaks are a confirming tool for the sidebands around line frequency and occur at:

$$f_{swirl} = \left[1 - \left(\frac{2}{5}\right)ks\right] * 5 f_{Line} \qquad (5)$$

Where:

f_{swirl} is the location of the peaks around line frequency
k is the harmonic index 1,2,3...
s is the slip
f_{Line} is the line frequency

3. Inductance Measurements on Motors.

To measure the inductance, impedance is measured on each phase by applying a low-voltage AC signal of known frequency to the winding and measuring the current that is passed through the windings. Resistance of the windings is measured by applying a DC voltage to the windings and measuring the resulting current. From these measurements, inductance is calculated using Equation 6.

$$\mathrm{L} = \frac{X_L}{\omega} = \frac{\sqrt{\left(\frac{V_{ac}}{I_{ac}}\right)^2 - \left(\frac{V_{dc}}{I_{dc}}\right)^2}}{2\pi f} \qquad (6)$$

Where:

L is the inductance in Henries
X_L is the inductive reactance in Ohms
ω is 2πf
V_{ac} is the voltage of the AC test signal in Volts
I_{ac} is the current of the AC test signal in Amps
V_{dc} is the voltage of the DC test signal in Volts
I_{dc} is the current of the DC test signal in Amps
f is the frequency of the test signal in Hertz

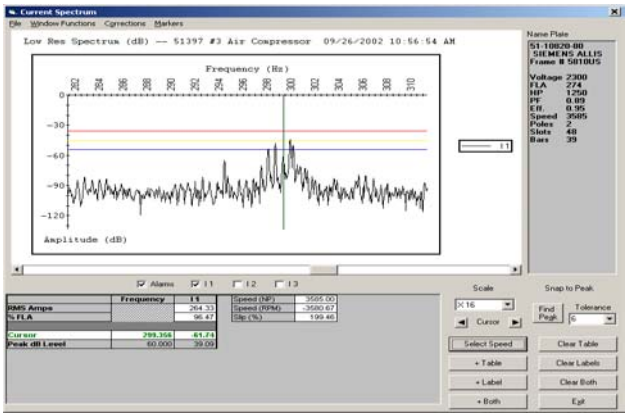

Figure 10. Swirl Effect

4. Physical Parameters That Affect Inductance

Several physical parameters affect inductance; these include the area of the core, number of turns, length of the air gap, length of the magnetic circuit, and the incremental permeability of the steel, as indicated in Equation 7. In a motor, the number of turns, area of the core, and the length of the magnetic circuit are constant. The primary parameter that will affect the inductance is the length of the air gap. Another parameter that affects the inductance to a far lesser degree than the air gap is the incremental permeability of the steel, especially at the low flux densities used in the inductance measurements. Effects from fringing flux are not included in this formula for simplicity.

$$\mathrm{L} = \frac{3.19 N^2 A_c \text{ x } 10^{-8}}{l_g + \frac{l_m}{\mu_\Delta}} \qquad (7)$$

Where:

L is the inductance in Henries
N is the number of turns
A_c is the area of the core in square inches
l_g is the length of the air gap in inches
l_m is the length of the magnetic path in inches
μ_Δ is the incremental permeability

5. Influence of the Rotor on the Measurement of Inductance

Seen in the past as a nuisance, the influence of the rotor on the measured inductance offers advantages in detecting the health of a motor. Plotting measured inductance with respect to rotor position (rotation) provides a valuable tool to determine the health of the motor. In this test, the rotor is rotated in discrete increments, and the inductance is measured at each point. The resulting graph of inductance will typically display waveforms sinusoidal in shape. These waveforms may then be analyzed to determine the overall health of the rotor and stator.

6. Analyzing Inductance Waveforms

When analyzing inductance waveforms, there are three main factors to consider, the amplitude of the inductance waveforms, repeated variations in the waveforms throughout all three phases, and the phasing of the waveforms. The amplitude of inductance waveforms depends on the type of motor, its construction, the residual flux on the rotor, and the overall health of the motor. Low amplitudes with very little sinusoidal activity of the inductance waveforms indicate the rotor is of "low influence." Low Influence Rotors (LIR) are typically higher quality, have copper bars, and have no defects (see Figure 11).

Figure 11. Inductance Test of a Rotor With "Low Influence"

An increase in the amplitude of the inductance waveforms often indicates a developing fault in the motor, especially in rotors that initially have low influence. Rotors that are porous cast aluminum or that have adverse conditions such as broken or cracked rotor bars produce these effects. As the severity of the fault increases, the amplitudes of the waveforms increase and the waveforms will become sinusoidal in shape (see Figure 12). A baseline test should be performed prior to installation of the motor or as early as practical. Once a baseline test has been established, the motor should be monitored for trends of increasing amplitude and sinusoidal development of the inductance waveforms.

Figure 12. Inductance Test of a Rotor "With Influence"

Repeated variations throughout all three phases of inductance waveforms are a very good indicator of developing faults in the rotor as shown in Figure 13. Repeated variations are caused by the reflected impedance of the cage and the increase in residual flux on the rotor. Evaluate all three inductance waveforms for these repeated variations.

Figure 13. Repeated Variations Throughout All Three Phases of Inductance

Lastly, evaluate the waveforms for phasing differences. Phasing differences occur when the peak of one waveform will be shifted in phase.

7. Inductive Imbalance

Using the inductance measurements, percent (%) inductive imbalance is calculated as follows:

$$\%L_{imb} = \frac{\Delta_{\max}}{L_{avg}} \text{ x } 100\% \qquad (8)$$

Where:

$\%\ L_{imb}$ is the inductive imbalance in percent

Δ_{max} is the maximum deviation of inductance from the average inductance in Henries

L_{avg} is the average inductance in Henries

Percent inductive imbalance is used to determine how well the winding impedances are balanced. Although no specific standards have been established due to the influence of the rotor on the measurement of inductance, in a healthy motor it is generally accepted there should be less than a 7% inductive imbalance for form wound motors and less than 12% for random wound motors. Some rotors have half of the cage shifted at the center of the rotor, which, from our experience, tends to create an inductive imbalance of approximately 8 to 15% between phases.

III. SUMMARY

Using fault zone analysis approach provides a more complete analysis of motor health. This approach analyzes the Power Quality, Power Circuit, Stator, Air Gap, Insulation, and Rotor fault zones of your electric motor. All six fault zones should be analyzed to accurately assess the overall health of your motor.

REFERENCES

P. Bechard, “Advanced Spectral Analysis,” NETA World, Summer 2004.

N. Bethel, “Identifying Motor Defects Through Fault Zone Analysis,” Enteract ’98 Conference, April 1998.

S. J. Chapman, *Electric Machinery Fundamentals*. McGraw-Hill Publishing Company, 1985.

G. B. Kliman, A. V. Mohan Rao, “Broken Bar Detector for Squirrel Cage Induction Motors,” GE Company Report, 1986.

G. B. Kliman, J. Stein, R. D. Endicott, and M.W. Madden, “Noninvasive Detection of Broken Rotor Bars in Operating Induction Motors,” *IEEE Transactions on Energy Conversion*, Vol. 3, No. 4, December 1988.

D. McKinnon, H. Smolleck, “Influence of Rotor Residual Flux on the Measurement of Inductance and its possible use as an Impending Fault Indicator,” IEEE EMCW 2004 Technical Conference, September 2004.

Jafar Milimonfared, Homayoun Meshgin Kelk, Subhasis Nandi, Student Member, IEEE, Artin Der Minassians, Member, IEEE, and Hamid A. Toliyat, Senior Member, IEEE. “A Novel Approach for Broken-Rotor-Bar Detection in Cage Induction Motors,” *IEEE Transactions on Industry Applications*, Vol. 35, No. 5, September/October 1999.

S. Smith, *Magnetic Components Design and Applications*. Van Nostrand Reinhold Company, 1985.

David L. McKinnon received his BS in Electrical Engineering from New Mexico State University in 1991 and a MBA from the University of Phoenix in 2002. He has worked in the field of magnetics for over 12 years. During the past three years, he has worked for PdMA Corporation as a Project Manager for hardware and product development of motor test equipment.